

(1968); (b) R. A. Marcus, *J. Am. Chem. Soc.*, **91**, 7224 (1969).

(27) (a) W. J. Albery, *Pure Appl. Chem.*, **51**, 949 (1979); (b) E.

S. Lewis and S. J. Kukes, *J. Am. Chem. Soc.*, **101**, 417 (1979).

(28) R. A. Marcus, *J. Phys. Chem.*, **72**, 891 (1968).

A Kinetic Study of Br Atom Reactions with Trimethylsilane by the VLPR (Very Low Pressure Reactor) Technique¹

Kwang Yul Choo[†] and Mu Hyun Choe

Department of Chemistry, College of Natural Sciences, Seoul National University, Seoul 151, Korea
(Received January 30, 1985)

A Very Low Pressure Reactor (VLPR) is constructed for the kinetic study of atom-molecule bimolecular elementary reactions. The basic principles and the versatility of the method are described. By using the VLPR technique the forward (k_1) and the reverse (k_{-1}) rate constants for Br atom reaction with trimethylsilane are studied; $\text{Br}\cdot + (\text{CH}_3)_3\text{SiH} \xrightleftharpoons[k_{-1}]{k_1} \text{HBr} + (\text{CH}_3)_3\text{Si}\cdot$. From the kinetic data and the entropy estimation the bond dissociation energy for Si-H bond in trimethylsilane is calculated to be 90.1 kcal/mole (± 1.1 kcal/mole). The Arrhenius parameters for k_1 are found to be $\log A = 10.6$ l/mole·sec, $E_a = 4.4$ kcal/mole respectively. For the comparison purpose analogous reaction for carbon compound; $\text{Br}\cdot + (\text{CH}_3)_3\text{CH} \rightarrow \text{HBr} + (\text{CH}_3)_3\text{C}\cdot$ was also studied. The corresponding rate constant and equilibrium constant at 25°C are found to be 2.67×10^6 l/mole·sec and 160 respectively.

Introduction

The greater size and reduced electronegativity of the silicon atom along with the possibility of d-orbital participation cause silicon compounds to behave abnormally in comparison with their carbon analogs, although carbon and silicon both belong to the same group (group IV) in the periodic table. It has been generally accepted that silicon-silicon, silicon-carbon, and silicon-hydrogen bonds are weaker than carbon-carbon, and carbon-hydrogen bonds, respectively.

Recently the kinetic and mechanistic study of silicon compounds gained wide interests due mainly to their unusual properties in comparison with their carbon analogs. The generation and detection of silicon-centered free radicals², divalent silicon species³, and double bonded (Si=R, R=O, Si, C) silicon compounds⁴ has been one of the most exciting research areas in organosilicon chemistry. Because of the complexity of silicon chemistry a detailed kinetic and thermochemical parameters for reactive silicon intermediates should be known to account for complex silicon reactions properly. It would be interesting to compare the chemistry of silicon compounds with that of carbon analogs to shed light on the similarities and/or differences between those two classes of compounds.

Indirect determinations of rate constants for the elementary gas phase reactions of halogen atoms with various hydrocarbons have been carried out during the last few decades. Only recently a direct determination of the rate constants has been published. Most of the workers have used atomic absorption,⁵ atomic fluorescence,⁶ and ESR technique⁷ for the detection of halogen atoms, and reaction times were usually determined by a flow or a pulse method. The drawbacks of these methods for general determination of kinetic parameters are well known; (1) the detector only detects the reactive intermediates and no

information on all the products can be obtained, (2) the species interested should have suitable spectroscopic transitions in the proper spectral range, and (3) the reactants should be inert with the flash light that is used for the generation of reactive intermediates.

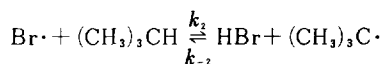
We have recently constructed a Very Low Pressure Reactor (VLPR) kinetic system which is more general than the known methods for the study of elementary reaction kinetics. The system consists of the very low pressure Knudsen reactor and molecular-beam mass spectrometric detection unit by which all the reactants and products can be detected without the complication of secondary reactions. By using the Knudsen cell reactor the absolute rate constants can be directly deduced. Successful applications of the Knudsen cell reactor system for unimolecular elementary kinetics have been reported.⁸

Br atom reaction with trimethylsilane, $\text{Br}\cdot + (\text{CH}_3)_3\text{SiH} \xrightarrow{k_1}$, is one of the elementary reactions for the bromination of silane. Since we can also measure the reverse rate constant, *i.e.* $\text{HBr} + (\text{CH}_3)_3\text{Si}\cdot \xrightarrow{k_{-1}}$, by using our VLPR system, the Si-H bond dissociation energy of $(\text{CH}_3)_3\text{SiH}$ can be estimated from the rate constants. There have been continuous controversy over the exact bond dissociation energy of Si-H bond in trimethylsilane. Reported values range from ca. 75 kcal/mole⁹ to 89.8 kcal/mole.¹⁴

The purpose of this research is to measure the elementary reaction rate constants for the Br atom reaction with trimethylsilane and trimethylsilyl radical with HBr (k_1 and k_{-1}). From the rate data the bond dissociation energy for Si-H bond was estimated.

Although the kinetic measurements of Si-H bond energy in trimethylsilane was recently reported in our laboratory as a preliminary form¹ here we included a detailed description of

our experimental set-up and kinetic analyses for the VLPR technique and silicon reaction system. For the comparison purpose Br atom reaction with isobutane, a carbon analog of trimethylsilane, was also studied;



Experimental

Materials. Trimethylsilane was purchased from PCR, Inc. and used without further purification. HBr, Helium and isobutane were obtained from Matheson and used after trapping high boiling impurities. Br₂ was from Kanto Chem. Co., and used after several freeze-thaw treatments.

We found no mass spectroscopically detectable impurities in all the chemicals used in this experiment.

The Very Low Pressure Reactor

Figure 1 shows the schematic drawing of the stainless steel Very Low Pressure Reactor (VLPR). Under ordinary experimental conditions the pressure in the reactor is in the range of 10⁻²~10⁻⁴ torr.

The Knudsen cell reactor is characterized by the collision number,

$$Z_w = A_w/A_h$$

A_w is the surface area of the wall of reactor and *A_h* is the area of the escape hole. *Z_w* is the average number of collisions with the walls made by a molecule during its residence time in the reactor. The characteristic collision number of our reactor is 5070. Under our experimental conditions the collision frequency of a molecule with wall is ca. 10³ and with other molecule is ca. 10².

The average residence time, *t_r*, of the molecule of mass *M* in the reactor is given by the Knudsen equation¹¹ as,

$$t_r = \frac{4V}{\bar{c} A_h} \text{ sec}$$

where *V* is the volume of the reactor in cm³, and *c* is the mean molecular speed given by kinetic theory as,

$$\bar{c} = \left(\frac{8RT}{\pi M}\right)^{\frac{1}{2}} = 1.46 \times 10^4 (T/M)^{\frac{1}{2}} \text{ cm/sec}$$

We can define first order rate constant, *k_{em}*, which characterizes the rate of escape of species of mass *M* from the reactor;

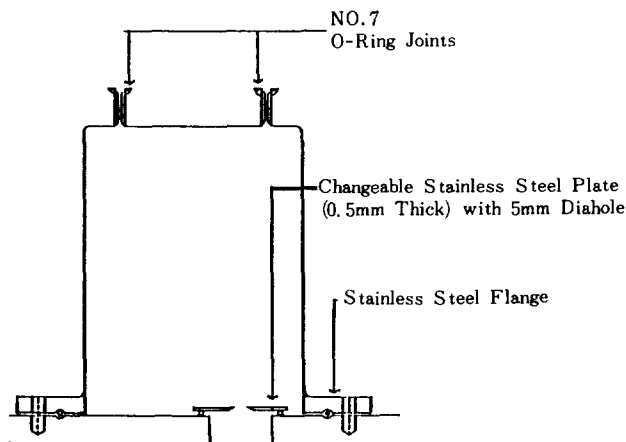


Figure 1. Stainless-steel Very Low Pressure Reactor.

$$k_{em} = \frac{1}{t_r} = 3.65 \times 10^3 (A_h/V) (T/M)^{\frac{1}{2}} \text{ sec}^{-1}$$

If *F_M* is the flux of molecules *M* into the reactor cell (molecules/sec), the steady state concentration of *M* in the reactor is given by,

$$M_{ss} = \frac{F_M}{V k_{em}} \text{ molecules/cm}^3$$

The volume, *V*, and escape hole area, *A_h*, of our VLPR cell are 2.14 × 10³ cm³ and 0.181 cm² respectively.

Under VLPR condition,

$$\begin{aligned} -\frac{d(M)}{dt} &= k_{em}(M) \\ \ln(M) &= \ln(M)_0 - k_{em} \cdot t \end{aligned}$$

Thus, the plot of the logarithm of spectral intensity, *ln(M)*, against time, *t*, gives a straight line. The experimentally determined *k_{em}*'s at different temperatures are found to be in good agreement with calculated values from the reactor geometry and Knudsen equation. The *k_{em}* for our reactor is

$$k_{em} = 2.99 \times 10^{-1} \left(\frac{T}{M}\right) \text{ sec}^{-1}$$

At 298 K, trimethylsilane has the escape rate constant, *k_{em}*, of 0.599 sec⁻¹ and the residence time, *t_r*, of 1.67 sec. From the residence time and the characteristic collision number of our reactor, the collision frequency (*Z_w/t_r*) of trimethylsilane with wall is calculated to be 3.04 × 10³ sec⁻¹.

For Br + (CH₃)₃CH reactions, the measurement of equilibrium constant and forward rate constant was carried out with the same reactor and analogous procedure as that of Br + (CH₃)₃SiH reactions.

General description of the kinetic system)

The system consists of two parts : the glass vacuum system and metal vacuum system. The glass vacuum system has sample reservoirs (51), flow measurement section for feeding sample molecules into reactor. The metal vacuum system has Very Low Pressure Reactor, mass spectrometer detection system, and differential pumping system.

A schematic representation of the metal vacuum system is shown in Figure 2. Molecular species, trimethylsilane and hydrogen bromide, are flowed into the reactor via a capillary entrance A, while the atomic species, Bromine atoms, generated

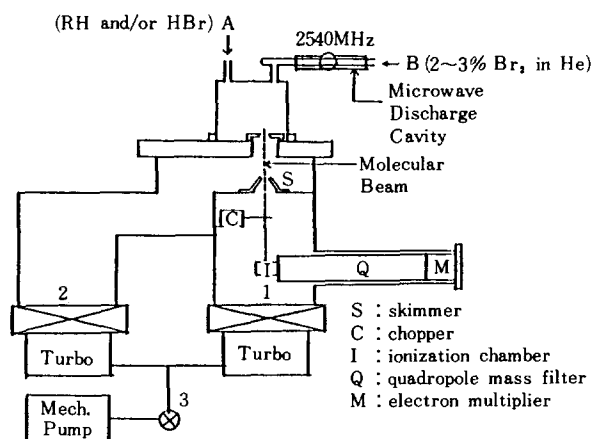


Figure 2. The Very Low Pressure Reactor and Associated Molecular Beam Mass Spectrometer System.

in the microwave (2540 MHz) discharge tube (Evanson type cavity with Kiva microwave generator, Kiva Inc., model MPG4), are leaked into the reactor via B through a pinhole. Being fed through capillary entrance, the molecular species have rare probabilities of back diffusion from the reactor. The inside wall of the reactor is coated with a halocarbon wax (Fluorocarbon Inc.) to prevent radical species from wall reactions such as hydrogen atom abstraction from the wall.

Chamber (1) and (2), are connected to gate valves (Varian Vacuum, model 951-5022) and turbomolecular pumps (Leybold-Heraeus Co., Turbovac 120 & 220). The pressure of chamber (1) and (2) are in the range of $10^{-5} \sim 10^{-6}$ torr and $10^{-7} \sim 10^{-8}$ torr respectively. The turbomolecular pumps share a common foreline, which is connected to a mechanical oil pump via an electromagnetic foreline valve (3).

The molecular beam mass spectrometer (UTI, model 100C) detection system analyzes the chopped molecular beam produced by the chopper. The chamber (1) is connected to the chamber (2) via a skimmer (hole diameter 1mm) which is located under the escape hole of the reactor. A tuning fork chopper (C) (Bulova watch Co. Inc., Type L20: Miniature) chops the molecular beam from the skimmer. After modulation the incoming molecular beam "pulses" reach the mass spectrometer ionizer (I), and are subsequently analyzed by the quadropole filter (Q) and detected by an electronmultiplier (M). The signal from the electronmultiplier is fed into a preamplifier located in the RF generator console. The amplified signal is then further fed into the lock-in amplifier (ITHACO Inc., model 393) which is locked to the frequency of the chopper (200 Hz). The processed mass spectral signals could be recorded either with X-Y recorder (Houston Inc., ser. 2000) or the storage oscilloscope (Tektronix Inc., model 5111).

The glass vacuum system has mechanical and diffusion pumps capable of pumping to an ultimate pressure of 1×10^{-5} torr. The flow rates of molecules were calculated by measuring the pressure drop/unit time with three pressure transducers (Vallydine Co., model DP7).

Results and Discussion

Figure 3 shows the molecular beam mass spectrum of Br atoms and Br_2 molecules with microwave discharge on and off respectively. As shown in the figure, when the discharge was

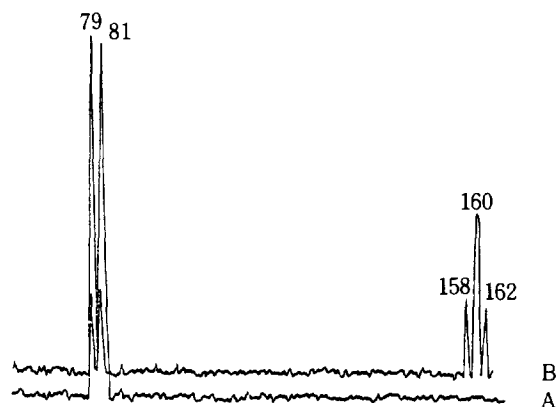


Figure 3. Dissociation of Br_2 molecules into Br Atoms by Microwave Discharge. A, with Discharge on B, with Discharge off.

on, all the Br_2 molecules were dissociated and all the Br atoms generated in the microwave discharge tube could survive as Br atoms after many collisions with the wall of reactor cell. The absence of Br_2 molecule (mass spectral signals at 158, 160, 162 amu) and HBr molecule (main spectral signals at 80, 82 amu) with discharge on indicates the recombination of Br atoms to form Br_2 and wall reaction of Br atoms to generate HBr are negligible under our experimental conditions. Without the wall coating with fluorocarbon wax HBr and Br_2 were the major mass spectral peaks instead of Br signal when the discharge was turned on.

To these Br atoms appropriate amount of trimethylsilane was added. Due to the reaction of Br atoms with Me_3SiH , the decrease of Br peaks at 79 and 81 amu and the increase of HBr peaks at 80 and 82 amu could be observed. This behavior is shown in Figure 4. In actual experiment we recorded the mass spectrum of the Br atom signal at 79 amu, and observed the

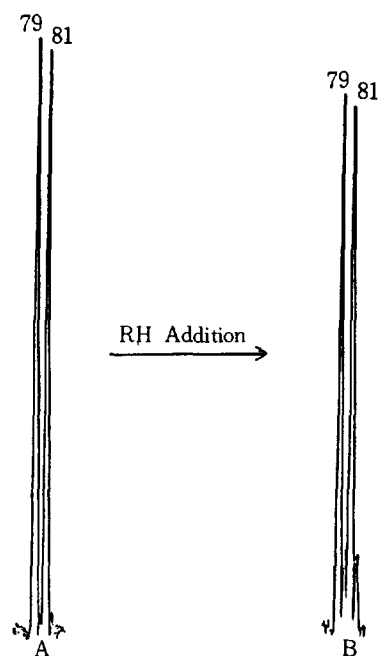


Figure 4. Decrease of Br Atom Signal and Appearance of HBr Signal with the Addition of RH.

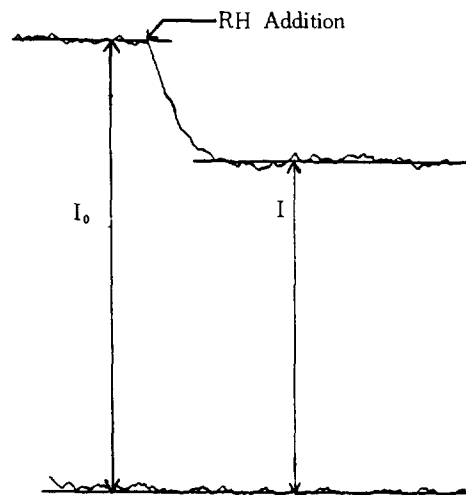
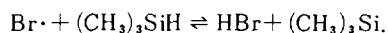


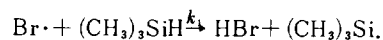
Figure 5. Mass Spectrometrical Measurement of Br Atom Concentration for Kinetics. I_0 , Br Atom Intensity without the addition of RH, I , Br Atom Intensity with the addition of RH.

decrease of it as shown in Figure 5.

Under usual experimental conditions (no excess trimethylsilane) HBr and R· were the main product signals, which indicates negligible secondary reactions.



The absolute rate constant for the forward reaction,



can be obtained from the steady state treatment of species involved;

$$\frac{d(\text{Br}\cdot)}{dt} = 0 = \frac{F_{\text{Br}}}{V} - k_1(\text{Br}\cdot)(\text{Me}_3\text{SiH}) - k_{\text{eBr}}(\text{Br}\cdot)$$

F_{Br} = Br atom flux into the reactor.

V = volume of the reactor.

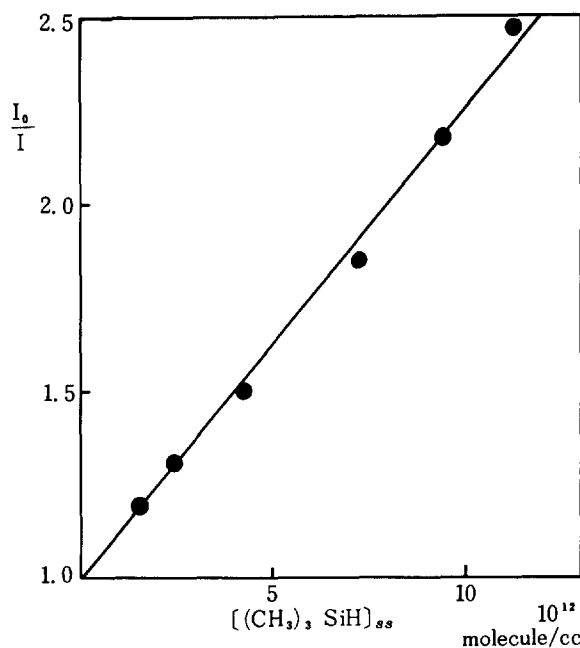


Figure 6. Forward Reaction Rate Constant, k_1 , of $\text{Br}\cdot + \text{HSiMe}_3$ Reaction at 33°C.

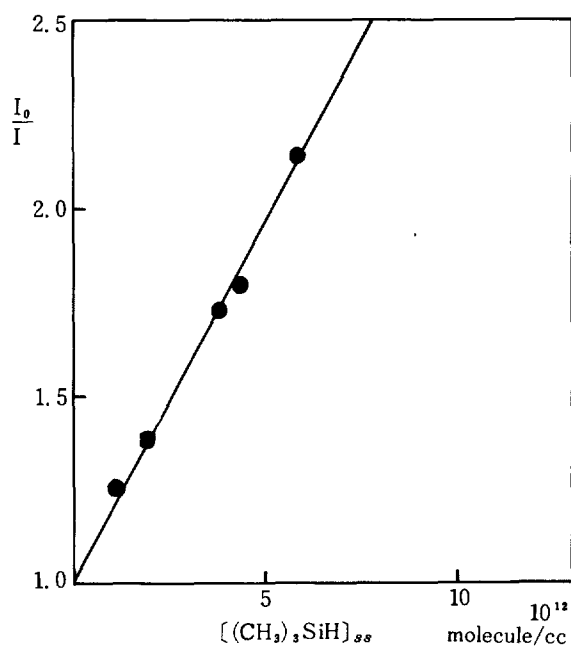


Figure 7. Same as Figure 6 at 40°C.

therefore, $\frac{F_{\text{Br}}}{V} = k_{\text{eBr}}(\text{Br}\cdot)_0$

$(\text{Br}\cdot)_0$ = Br atom concentration without the addition of trimethylsilane.

$(\text{Br}\cdot)$ = Br atom concentration with the addition of trimethylsilane.

After dividing the equation with $k_1(\text{Br}\cdot)$ and rearrangement, we get,

$$\frac{(\text{Br}\cdot)_0}{(\text{Br}\cdot)} = 1 + \frac{k_1(\text{Me}_3\text{SiH})}{k_{\text{eBr}}}$$

As the mass spectral signal intensity, I , is proportional to the concentration in the reactor,

$$\frac{(\text{Br}\cdot)_0}{(\text{Br}\cdot)} = \frac{I_0}{I} = 1 + \frac{k_1(\text{Me}_3\text{SiH})}{k_{\text{eBr}}}$$

Therefore, by plotting I_0/I against (Me_3SiH) , one can obtain k_1/k_{eBr} from the slope of the plot which should give intercept 1. Since k_{eBr} is constant under a given experimental condition k_1 can be obtained directly from the experiment.

Figure 6 and 7, and Table 1 show the experimental data obtained. A reasonable linearity of the plot with predicted intercept indicates the general validity of our method. Table 1 gives the k_1 values at different temperatures. Since we expect negligible difference in A factor between $\text{Br}\cdot + \text{Me}_3\text{CH} \rightarrow$ reaction and analogous $\text{Br}\cdot + \text{Me}_3\text{SiH} \rightarrow$ reaction,¹² the A factor for Br atom reactions with trimethyl silane (H atom abstraction reaction) can be reasonably assumed to be $\log A = 10.6 \pm 0.5$ ($l \cdot \text{mole}^{-1} \cdot \text{sec}^{-1}$).¹³

TABLE 1: Forward Reaction Rate Constant, k_1 , at Various Temperatures for $\text{BR}\cdot + \text{Me}_3\text{SiH}$ Reaction

Temperature °C	k_1 10^7 $l \cdot \text{mole}^{-1} \text{sec}^{-1}$
26	3.36
33	4.45
40	6.72
55	9.20

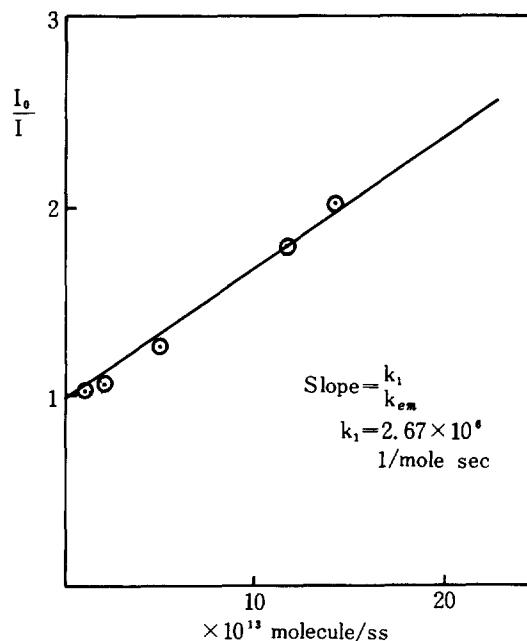
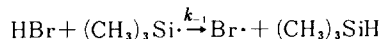


Figure 8. Forward Reaction Rate Constant, k_1 , for $\text{Br}\cdot + \text{HCMe}_3$ Reaction at 25°C.

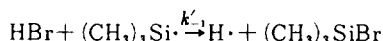
With this A factor and k_1 values at different temperatures the Arrhenius activation energy, E_a , for the process was estimated to be 4.4 ± 0.4 kcal/mole. Figure 8 shows similar plot for isobutane.

At 298°K the forward rate constant and equilibrium constant for $\text{Br}\cdot + (\text{CH}_3)_3\text{CH} \rightleftharpoons \text{HBr} + (\text{CH}_3)_3\text{C}\cdot$ were determined to be 2.67×10^6 l/mol sec and 160 respectively.

The rate constant for the reverse reaction,



and the equilibrium constant for the reaction were measured by adding appropriate amount of HBr into the reactor in which $\text{Br}\cdot + \text{Me}_3\text{SiH}$ reaction is going on. It seemed quite surprising to note that the other possible channel of the reaction, *i.e.*,



did not contribute for the reaction of HBr with $\text{Me}_3\text{Si}\cdot$ considering the relatively stronger Si-Br bond energy compared to the C-Br bond.

This fact was confirmed by the increase of $\text{Br}\cdot$ concentration with the addition of HBr into the reactor, and the reduction of secondary reaction products of trimethylsilyl radical.

Under steady state condition the following equation can be written from reactions 1 and -1.

$$\frac{d(\text{Br}\cdot)}{dt} = 0 = \frac{F_{\text{Br}}}{V} - k_1(\text{Br}\cdot)(\text{Me}_3\text{SiH}) - k_{\text{eBr}}(\text{Br}\cdot) + k_{-1}(\text{HBr})(\text{Me}_3\text{Si}\cdot)$$

$$\frac{d(\text{Me}_3\text{Si}\cdot)}{dt} = 0 = k_1(\text{Br}\cdot)(\text{Me}_3\text{SiH}) - k_{-1}(\text{HBr})(\text{Me}_3\text{Si}\cdot) - k_{\text{eMe}_3\text{Si}}(\text{Me}_3\text{Si}\cdot)$$

By rearranging above equations the following equation can be obtained

$$\frac{(\text{Br}\cdot)}{(\text{Br}\cdot)_0 - (\text{Br}\cdot)} = \frac{I}{I_0 - I} = \frac{k_{\text{eBr}}}{k_1(\text{Me}_3\text{SiH})} + \frac{k_{-1}}{k_1} \frac{k_{\text{eBr}}}{k_{\text{eMe}_3\text{Si}}} \frac{(\text{HBr})}{(\text{Me}_3\text{SiH})}$$

Thus, by plotting $I/(I_0 - I)$ vs. $(\text{HBr})/(\text{Me}_3\text{SiH})$ we can obtain k_1 from the intercept and k_1/k_{-1} from the slope of the plot. If we use the k_1 value from the previous experiment, we can draw a straight line from the calculated (with given Me_3SiH concentration) intercept. From the slope of the plot and calculated values of $k_{\text{eMe}_3\text{Si}}$ and k_{eBr} , the equilibrium constant was calculated to be 0.854.

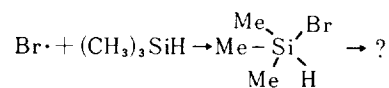
In our experiment, we could see a secondary reaction product of $\text{Me}_3\text{Si}\cdot$ when excessive trimethylsilane was flowed into the reactor. The mass spectral peaks at 152 and 154 were twin

TABLE 2: Thermochemical Parameters

Species	H_f° (kcal/mole)	S° (e.u.)
HBr	-8.7	47.5
Br	26.7	41.8
$(\text{CH}_3)_3\text{SiH}$	—	—
$(\text{CH}_3)_3\text{Si}\cdot$	—	—
$(\text{CH}_3)_3\text{Si}\cdot$	—	—
$(\text{CH}_3)_3\text{CH}$	-32.2	70.4
$(\text{CH}_3)_3\text{C}\cdot$	7.2~10.5	72.2

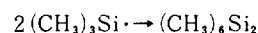
peaks indicating that they have a bromine atom as one of their constituent atoms. We tentatively identify this product as $(\text{CH}_3)_3\text{SiBr}$.

The studied reaction is H atom abstraction reaction by Br atom. For another possible mechanism, the displacement reaction by $\text{Br}\cdot$ can be postulated.



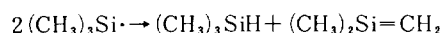
If pentavalent species were involved in the process, as shown above, the methyl radical, not hydrogen atom, would come out from pentavalent methyl silanes due to the relatively weak Si-C bond energy compared to Si-H bond energy, as Walsh *et al.* suggested in their paper.¹⁴ We have not seen any mass spectral signal from methane which indirectly indicates that pentavalent silicon intermediates were not formed in our experiment.

The evidence that the recombination reaction of $\text{Me}_3\text{Si}\cdot$ radical,



does not occur as a secondary reaction was given by the absence of mass spectral signal of the product, Me_6Si_2 , at 146 amu.

The kinetic study¹⁵ of the disproportionation reaction of $\text{Me}_3\text{Si}\cdot$,



indicated that its rate constant is smaller than the above recombination reaction by a factor of 0.48. Hence we can conclude it does not occur in our experiment.

Table 2 lists known thermochemical parameters for the species studied in this work. From the table and the thermochemical relationship, $\Delta G = \Delta H - T\Delta S = -RT \ln K$, the enthalpy of reaction can be obtained if we can calculate the entropy of reac-

TABLE 3: Bond Dissociation Energy of Si-H Bond in $(\text{CH}_3)_3\text{SiH}$ and the Arrhenius Parameters for $\text{Br}\cdot + (\text{CH}_3)_3\text{SiH}$ Reaction

(1) Bond Dissociation Energy	
Equilibrium Constant; $K = \frac{k_1}{k_{-1}} = 0.854$ (at 298°K)	
Entropy Change for $\text{Me}_3\text{SiH} \rightarrow \text{Me}_3\text{Si}\cdot$	
Contribution	ΔS
Spin ln 2	1.4 e.u.
Symmetry	0
Barrier	
($V = 1.7$ kcal/mole)	
→ Barrier (0)	2.4 e.u.
→ no change	0
$\Delta S = +1.4 \sim +3.8$ e.u. $= 2.6 \pm 1.2$ e.u. $D(\text{Me}_3\text{Si-H}) = 90.1 \pm 1.1$ kcal/mole	

(2) Arrhenius Parameters

A factor; assumed to be $\log A = 10.6 \pm 0.5$ ($l \cdot \text{mole}^{-1} \cdot \text{sec}^{-1}$)

E_a ; from Arrhenius plot $E_a = 4.4 \pm 0.4$ (kcal/mole)

$$k_1 = 10^{10.6 \pm 0.5} \exp \left\{ \frac{(4.4 \pm 0.4) \times 10^3}{RT} \right\}$$

TABLE 4: Arrhenius Parameters for H atom Transfer Reactions of Silicon and Carbon Compounds (A in l/(mole·mole), E_a in kcal/mole)

Radical	Substrate	log A	E_a	ref	Substrate	log A	E_a	ref
CH ₄	SiH ₄	8.8	7.0	12-a	CH ₄	9.0	14.9	13
	Si ₂ H ₆	9.0	5.6	12-a	C ₂ H ₆	9.3	12.1	13
	(CH ₃) ₃ SiH	8.3	7.8	21	(CH ₃) ₃ CH	8.5	8.2	13
CF ₃	SiH ₄	8.9	4.9	12-b	CH ₄	9.3	12.5	13
	(CH ₃) ₃ SiH	9.3	5.6	22	C ₂ H ₆	8.7	8.3	13
	(CH ₃) ₃ Si	8.6	7.2	13	(CH ₃) ₃ CD	9.2	7.4	13
Br	(CH ₃) ₃ SiH	10.6	4.4	This work	(CH ₃) ₃ C	8.7	8.4	13
					(CH ₃) ₃ CH	10.6	7.8	13
					(CH ₃) ₃ CH	10.6	7.0	This work
I	Cl ₃ SiH	10.9	21.4	23	(CH ₃) ₃ CH	10.9	21.4	13
	(CH ₃) ₃ SiH	10.9	19.7	14				
	(CH ₃) ₃ Si	11.8	29.2	24				

tion. The entropy change between trimethylsilyl radicals and trimethylsilane can be reasonably estimated by the method of Benson.¹⁶

Table 3 shows the estimation of entropy change and calculated bond dissociation energy of Si-H bond, $D(\text{Me}_3\text{Si-H})$. Arrhenius parameters, A and E_a , and the rate equation are listed together. For the estimation of entropy change the contribution from the change of translational, rotational and vibrational motions can be neglected. The entropy change caused by the difference of rotational barrier of methyl group was calculated with reference to that ($V = 1.7$ kcal/mole) of monomethylsilane (CH_3SiH_3) and dimethylsilane ($(\text{CH}_3)_2\text{SiH}_2$).¹⁶ The trimethylsilyl radical is reported to be a nonplanar radical,¹⁷ so the total symmetry (3^3) is the same as that of trimethylsilane. The increase in entropy originated from the spin degeneracy of odd electron is included in the calculation.

The calculated ΔG value for the reaction is 93.5 cal/mole and $T\Delta S$ is calculated to be 2.5 Kcal/mole. The uncertainty in $D(\text{Me}^3\text{Si-H})$ caused by the scatter of data points is ± 0.7 kcal/mole, and the uncertainty related to the assignment of rotational barrier of methyl group is ± 0.4 kcal/mole. With uncertainties stated above, we can reasonably conclude that the bond dissociation energy, $D(\text{Me}_3\text{Si-H})$, estimated from the experiment is 90.1 ± 1.1 kcal/mole.

There have been several reported measurement for the bond dissociation energy of methyl-substituted silanes. For $D(\text{Me}_3\text{Si-H})$ early experimental data of pyrolysis of Me_3SiH by Davidson and Lambert¹⁸ gave a value of 81 kcal/mole. With correlation curve of HT yield and bond dissociation energy obtained from recoil tritium abstraction reaction, Hosaka and Lowland¹⁹ predicted $D(\text{Me}_3\text{Si-H})$ as 85 kcal/mole. Hess, Lamp and Sommer²⁰ reported $D(\text{Me}_3\text{Si-H})$ to be 88 kcal/mole from the study of trimethylsilane ionization by electron impact method. Their value had an inherited uncertainty of ± 10 kcal/mole from the rough estimation of the heat of formation of hexamethyldisilane. Recently Walsh and Wells¹⁴ measured $D(\text{Me}_3\text{Si-H})$ with kinetic study of gas phase reaction of iodine and trimethylsilane. Their value was 89.0 ± 2.6 kcal/mole. In comparison with our result, 90.1 ± 1.1 kcal/mole, Walsh *et al.*'s value is in good agreement with our value within the error limit.

In Table 4, we list Arrhenius parameters for various hydrogen atom transfer reactions of silicon and carbon compounds. In the table we can easily recognize that the logarithms of A fac-

tors for a given radical reaction are identical (± 0.5 in log A , A is in units of $l \cdot \text{mole}^{-1} \cdot \text{sec}^{-1}$) with silicon and analogous carbon compounds. Activation energies of carbon compound series decrease as the number of the substituted methyl group increases, but in silicon compound series the trend is reversed as illustrated by the cases of SiH_4 and Me_3SiH . At the present time no firm explanation can be given for this unusual trend of activation energies in silicon hydrides. Apparently simple Evans-Polanyi type correlation, $E_a \propto D(\text{R-H})$, does not hold in silicon hydrides ($\text{R}_3\text{Si-H}$).

Acknowledgement. One of the authors (K. Y. Choo) expresses his sincere gratitude to the Department of Chemistry, University of Southern California, for the help in constructing the VLPR equipment. We are also indebted to the SNU-USAID Office, Seoul National University, for the equipment fund. This work was supported in part by a grant from the Ministry of Education.

References

- (1) This work has been appeared in preliminary form; M. Choe and K. Y. Choo, *Chem. Phys. Lett.* **89**, 115 (1982).
- (2) C. R. Park, S. A. Song, Y. E. Lee and K. Y. Choo, *J. Amer. Chem. Soc.*, **104**, 6445 (1982); K. Y. Choo and P. P. Gaspar, *J. Amer. Chem. Soc.*, **94**, 3032 (1972); **96**, 1284 (1974).
- (3) K. P. Steel and W. P. Weber, *J. Amer. Chem. Soc.*, **102**, 6095 (1980); W. D. Wuff, Goure, and T. J. Barton, *J. Amer. Chem. Soc.*, **100**, 6236 (1978).
- (4) R. T. Conlin and D. L. Wood, *J. Amer. Chem. Soc.*, **103**, 1843 (1981); T. J. Rahnak, J. Michl, and R. West, *J. Amer. Chem. Soc.*, **103**, 1845 (1981).
- (5) K. Y. Choo, P. P. Gaspar and A. P. Wolf, *J. Phys. Chem.*, **79**, 1752 (1975) and references there in.
- (6) J. V. Michael, D. F. Navam and L. J. Stief, *J. Chem. Phys.*, **70**, 1147 (1979).
- (7) A. Carrington, D. H. Levy and T. A. Miller, *J. Chem. Phys.*, **45**, 4093 (1966).
- (8) K. Y. Choo, D. M. Golden and S. W. Benson, *Int. J. Chem. Kinet.*, **7**, 713 (1975); **6**, 631 (1974); S. W. Benson and G. N. Spokes, *J. Amer. Chem. Soc.*, **89**, 2525 (1967); D. M. Golden, G. N. Spoken, and S. W. Benson, *Angew. Chem. Internat. Edit.*, **12**, 543 (1973); M. H. Baghal-Vayjooee, A. J. Cloussi, and S. W. Benson, *J. Amer. Chem. Soc.*, **100**, 3214 (1978).

- (9) E. V. A. Ebsworth, 'Volatile Silicon Compounds' Pergamon, London 1963.
- (10) F. E. Saalfeld and H. J. Svec, *J. Phys. Chem.*, **70**, 1753 (1966).
- (11) W. Kauzman 'Kinetic Theory of Gases' Benjamin, N.Y. 1966
- (12) (a) O. P. Strausz, E. Jakubowski, H.S. Sandhu and H. E. Gunning *J. Chem. Phys.*, **51**, 552 (1969); (b) *idem.*, *ibid.*, **52**, 4242 (1970); (c) K. Obi, H. S. Sandhu, H. E. Gunning and O. P. Strausz, *J. Phys. Chem.*, **76**, 3911 (1972).
- (13) C. H. Bamford ed. 'Comprehensive Chemical Kinetics' Elsevier, 1976 Vol. 18, p50, Table 7.
- (14) R. Walsh and J. M. Wells, *J. Chem. Soc., Faraday Trans. 1*, **72**, 100 (1976).
- (15) B. J. Cornett, K.Y. Choo and P. P. Gaspar, *J. Amer. Chem. Soc.*, **102**, 377 (1980); S.K. Tokach and R. D. Koob, *J. Phys. Chem.*, **83**, 774 (1979).
- (16) S. W. Benson, 'Thermochemical Kinetics' 2nd Ed. Wiley, N.Y. (1975).
- (17) H. J. Emelús and M. F. Lampert ed. 'MTP International Review of Science. Inorganic Chemistry. Series One. Vol. 1. Main Group Elements-Hydrogen and Group I-IV' Butterworths, London (1972); H. J. Emelús and d. B. Sowerby ed. 'Ibid. Series Two. Vol. 2. Main Group Elements-Group Elements-Group IV and V' (1975).
- (18) A. C. Baldwin, I.M.T. Davidson and M. D. Reed, *J. Chem. Soc., Faraday Trans. 1*, **74**, 2171 (1978); I.M.T. Davidson and C. A. Lambert, *J. Chem. Soc., A*, 882 (1971).
- (19) A. Hosaka and F. S. Rowland, *J. Phys. Chem.*, **77**, 705 (1973).
- (20) G.G. Hess, F.W. Lamp and Sommer, *J. Amer. Chem. Soc.*, **87**, 5327 (1965); W.C. Steele, L.P. Nichols and F.G.A. Stane, *J. Amer. Chem. Soc.*, **84**, 4441 (1962).
- (21) G. Baruch and A. Horowitz, *J. Phys. Chem.*, **84**, 2535 (1980).
- (22) E. R. Morris and J. C. Thynne, *Trans. Faraday Soc.*, **66**, 183 (1970).
- (23) R. Walsh and J. M. Wells, *J. Chem. Soc. Faraday Trans. 1*, **72**, 1212 (1976).
- (24) A. M. Doncaster and R. Walsh, *J. Chem. Soc. Faraday Trans. 1*, **72**, 2908 (1976).

Crystal Structure of Dehydrated Partially Ag⁺-Exchanged Zeolite A, Ag_{4.6}Na_{7.4}-A, Treated with Hydrogen at 350°C

Yang Kim

Chemistry Department, Pusan National University, Pusan 607, Korea

Karl Seff

Chemistry Department, University of Hawaii, Honolulu, Hawaii 96822, U.S.A. (Received February 22, 1985)

The crystal structure of Ag_{4.6}Na_{7.4}-A, dehydrated, treated with H₂, and evacuated, all at 350°C, has been determined by single crystal x-ray diffraction methods in the cubic space group *Pm3m* at 24(1)°C; *a* = 12.208(2)Å. The structure was refined to the final error indices *R*₁ = 0.088 and *R*₂ (weighted) = 0.069 using 194 independent reflections for which *I*_o > 3σ(*I*_o). On threefold axes near the centers of 6-oxygen rings, 7.4 Na⁺ ions and 0.6 Ag⁺ ions are found. Two non-equivalent 8-ring Ag⁺ ions are found off the 8-ring planes, each containing about 0.6 Ag⁺ ions. Three non-equivalent Ag atom positions are found in the large cavity, each containing about 0.6 Ag atoms. This crystallographic analysis may be interpreted to indicate that 0.6 (Ag₆)³⁺ clusters are present in each large cavity. This cluster may be viewed as a nearly linear trisilver molecule (Ag₃)⁰ (bond lengths, 2.92 and 2.94 Å; angle, 153°) stabilized by the coordination of each atom to a Ag⁺ ion at 3.30, 3.33, and 3.43 Å, respectively. In addition, one of the silver atoms approaches all of the 0(1) oxygens of a 4-ring at 2.76Å. Altogether 7.4 Na⁺ ions, 1.8 Ag⁺ ions, and 1.8 Ag atoms are located per unit cell. The remaining 1.0 Ag⁺ ion has been reduced and has migrated out of the zeolite framework to form silver crystallites on the surface of the zeolite single crystal.

Introduction

The structures of metal clusters are of great interest because of their pronounced catalytic activity.

Ag⁺ ions in zeolite A are autoreduced upon dehydration to form uncharged silver clusters, the molecules Ag₆, each within a cube of eight Ag⁺ ions, each near the plane of a 6-oxygen

ring.^{1,2} The number of silver clusters in 7 separate crystallographic determinations has been found to depend upon the dehydration time and temperature.² Hermerschmidt and Haul also identified these clusters in dehydrated Ag⁺-exchanged zeolite A using epr spectroscopy.³ These clusters, of (Ag₆)⁰ stabilized by coordination to 8 Ag⁺ ions, may also be viewed